Energy Proceedings
Vol 34, 2023
ISSN 2004-2965

An analytical method for evaluating the underground hydrogen storage capacity in depleted gas reservoirs using CO_2 as cushion gas

Youwei He[1*], Yu Qiao[1], Yong Tang[1], Guoqing Zhao[1]

1 State Key Laboratory of Oil and Gas Reservoir Geology and Exploitation, Southwest Petroleum University, Chengdu, Sichuan 610500, China

(*Youwei He: Youwei.he@163.com)

ABSTRACT

Underground hydrogen storage (UHS) is an effective means to solve large-scale energy storage. The depleted gas reservoirs can be used as the potential targets for UHS due to its huge storage space, good sealing ability, and the existing facilities. CO_2 can be injected as the cushion gas to reduce the loss of hydrogen and achieve carbon sequestration. This work proposes a novel analytical method to calculate the hydrogen storage capacity in depleted gas reservoirs using CO_2 as cushion gas considering hydrogen storage safety and gas (e.g., CO_2, H_2, CH_4) dissolution in formation water. The multi-components (H_2-CO_2-CH_4-H_2O) material balance equations are further developed by considering the edge/bottom water and gas dissolution in water as well as caprock breakthrough and fault instability. The maximum operating pressure of UHS is determined by calculating the caprock-breakthrough pressure and the fault-instability pressure. The proposed method has been applied to evaluate the UHS capacity of a depleted gas reservoir in the Sichuan Basin of China. The maximum pressure threshold of formation is determined to be 42M. The hydrogen storage capacity under different CO_2 cushion gas volume conditions is calculated. The study compares with the model without considering dissolution, and the influence of sensitive factors such as temperature and pressure on hydrogen storage capacity is analyzed.

Keywords: UHS, CO_2, cushion gas, material balance, storage capacity, depleted gas reservoir

NONMENCLATURE

Abbreviations	
UHS	Underground hydrogen storage
UGS	underground gas storage
SF	safety index

Symbols	
a	The proportion of CO_2 occupying the gas-bearing pore space of the formation
α	The dip angle of the fault plane
b	The proportion of CH_4 occupying the gas-bearing pore space of the formation
B_i	Natural gas volume coefficient under initial formation conditions
B_w	Formation water volume coefficient in the process of injection
B_{w_dep}	Formation water volume coefficient in the state of depleted gas reservoir
B_{wi}	The initial formation water volume coefficient
c	The proportion of H_2 occupying the gas-bearing pore space of the formation
c'	The cohesion force
c_{eff}	Effective compression coefficient
c_f	Coefficient of rock compression
c_w	Coefficient of water compression
ϕ	The internal friction angle
G_i	Original geological reserves of gas reservoir
M	Water body multiples
p	Formation pressure
p_{dep}	Depleted gas reservoir formation pressure
p_i	The initial formation pressure
p_{sc}	Standard pressure
σ	The positive stress perpendicular to the fault plane
σ_h	The minimum principal stress
σ_H	The maximum principal stress
σ_n	The effective positive stress
σ_1	The maximum effective principal stress
σ_3	The minimum effective principal stress
R	Ideal gas constant
R_{CO2}	The CO_2 solubility in formation water

This is a paper for International CCUS Conference 2023 (ICCUSC2023), April 14-15, 2023, Beijing, China.

R_H	The CH_4 solubility in formation water
R_{H_dep}	The CH_4 solubility in the state of depleted gas reservoir
R_{H2}	The H_2 solubility in formation water
Sw	The water saturation
T	Formation temperature
T_{dep}	Depleted gas reservoir formation temperature
T_i	The initial formation temperature
T_{sc}	Standard temperature
τ	The fault shear stress
τ_m	The maximum shear stress at a certain stress state
τ_m^*	The critical shear stress when the shear failure occurs
τ_s	The shear stress along the fault plane under a certain stress state
V	Formation hydrocarbon volume
V_{CO2}	The volume of CO_2 in the formation,
V_{CO2_dis}	The volume of dissolved CO_2
V_{CO2_inj}	The volume of injected CO_2
V_{dep}	The gas-bearing pore space in the formation under depleted formation conditions
V_{dep_dis}	The volume of natural gas dissolved in the depleted gas reservoir formation
V_H	The volume of natural gas in the gas reservoir formation
V_{H_dep}	The volume of natural gas in the depleted gas reservoir formation
V_{H_dis}	The volume of natural gas dissolved in the formation
V_{H2}	The volume of H_2 in the formation pore
V_{H2_dis}	The volume of dissolved H_2 in the formation
V_{H2_inj}	The volume of injected H_2
V_i	The gas-bearing pore space in the formation under initial conditions
V_w	Water volume under formation conditions
V_{w_p}	Water production volume
W_e	The water intrusion volume in the process of injection
W_{e_dep}	The water intrusion volume in the depleted formation condition
χ	The cap safety factor
Z_{CO2}	CO_2 deviation factor
Z_H	CH_4 deviation factor under formation conditions
Z_{H_dep}	CH_4 deviation factor under original formation condition
Z_{H2}	H_2 deviation factor,
Z_i	The initial formation natural gas deviation factor
Z_{sc}	Deviation factor under standard condition

1. INTRODUCTION

The hydrogen energy is a renewable, high-power and high-efficiency energy carrier, which is convenient for storage and conversion[1-4]. China's solar power and wind power industry is large in scale[5-6], but these two types of power utilization are low, and the waste electricity cannot be utilized[7]. The hydrogen energy becomes a favorable energy conversion carrier. By 2035, a hydrogen energy industry system will be formed, and a diversified hydrogen energy application ecology covering transportation, energy storage, industry and other fields will be built[8], as shown in Fig. 1. Along with the implementation of the "carbon neutrality, carbon emissions peak" policy, the hydrogen energy will play an important role as a clean energy source[9-10].

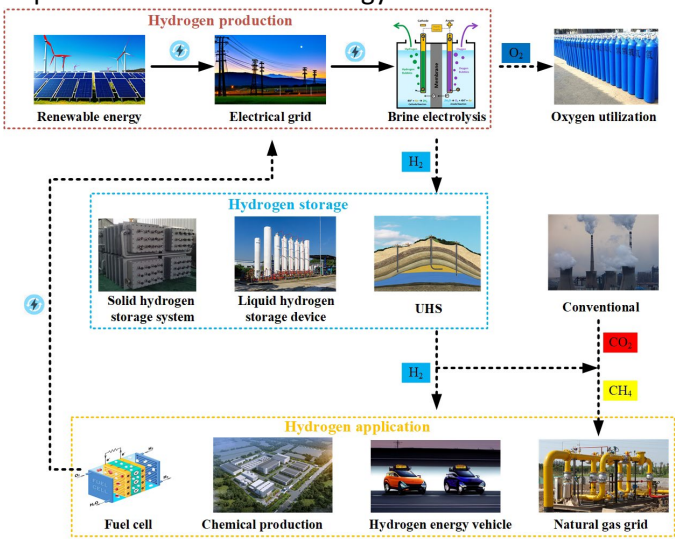

Fig. 1 The mode of production, storage and utilization of hydrogen energy

The hydrogen energy storage is mainly divided into the physical hydrogen storage and the chemical hydrogen storage[11]. The physical hydrogen storage mainly includes high-pressure gaseous hydrogen storage, low-temperature liquid hydrogen storage, activated carbon adsorption hydrogen storage, carbon fiber and carbon nanotube hydrogen storage, and underground hydrogen storage. The chemical hydrogen storage mainly includes metal hydride hydrogen storage, liquid organic hydrogen carrier hydrogen storage, inorganic hydrogen storage, and liquid ammonia hydrogen storage. The UHS is an effective way of large-capacity and long-term energy storage[11-13]. Similar to underground gas storage (UGS), natural gas is often stored in depleted oil and gas reservoirs, aquifers, salt

caverns and some abandoned pit caverns. But there are higher requirements for UHS, and the focus of the UHS research is to store hydrogen in depleted gas reservoirs and salt caverns[12, 14-16]. The UHS in depleted gas reservoir has the advantages of large volume, high geological awareness, good sealing and wide geographical distribution[15, 17-21]; the depleted gas reservoir usually contains a certain volume of residual gas, which can be used as cushion gas; meanwhile, the underground and surface original facilities can be partially utilized to reduce the investment cost of the UHS construction[22].

The development of UHS technology is an effective way to overcome the volatility and intermittency of renewable energy. The hydrogen storage capacity is a key factor for design engineers to consider and is an important indicator of the performance of the UHS. It is important to account for the volume of hydrogen stored in the UHS in real time and to determine the working gas volume at different pressures. Depleted gas reservoirs are the most common and economical form of building the UHS. Replacing valuable primary cushion gas with cheap CO_2 not only reduces the loss of hydrogen but also achieves the purpose of carbon storage[21, 23]. The construction of UHS with CO_2 as cushion gas not only achieves carbon emission reduction, but also improves the utilization of low-carbon energy[24-27]. Compared with the primary cushion gas and N_2, CO_2 has stronger compressibility, which can improve the CO_2 storage capacity of depleted gas reservoirs and enhance the hydrogen recovery efficiency in the process of hydrogen extraction[28-29]. However, the existing UHS capacity evaluation method cannot accurately evaluate the hydrogen storage capacity in porous media of depleted gas reservoirs using CO_2 as cushion gas. When CO_2 is used as the cushion gas of the UHS of the depleted gas reservoir, it needs to consider the equilibrium relationship of H_2-CO_2-CH_4 multi-component so that the hydrogen storage capacity of this reservoir can be evaluated more accurately.

At present, the UHS with CO_2 as cushion gas has not been really applied in the depleted gas reservoirs, and it is in the stage of simulation and experimental research. Hagemann et al. [30] simulated the injection of H_2 and CH_4 into porous media respectively, and pointed out that the displacement was uniform for low injection rate; When the injection rate is high, the viscous force becomes dominant, and the displacement becomes unstable. The lateral diffusion rate of H_2 is faster than that of CH_4, and the influence of microorganisms on UHS is considered. Pfeiffer et al.[31] simulated UHS in heterogeneous sandstone with N_2 as cushion gas. Lysyy et al. [19] pointed out that the thin gas area is the first choice for pure hydrogen storage, and it is not recommended to store hydrogen in water area. When only pure hydrogen is injected, most of the injected H_2 remains underground as cushion gas; Injecting formation gas as cushion gas leads to higher hydrogen recovery. Enigbokan et al. [21] used CO_2 as cushion gas to simulate the UHS in depleted gas field. The success factor of seasonal storage is that the injected hydrogen can remain closed before extraction. Eddaoui et al[32] pointed out that biological blockage in UHS is not only bad, but bacteria accumulate in places with high hydrogen saturation, forcing hydrogen to change its path and move in different directions. Bo et al. 2023[33] suggested that the relative permeability curve of hydrogen-brine obtained from experiments should be used when simulating UHS, in order to make the simulation results more robust.

For the capacity calculation of UHS, we could compare with the previous research methods on underground storage of other gases, such as gas storage and CO_2 storage. Yang et al. [34] adopted the advanced material balance method to calculate the dynamic reserves of gas reservoirs, and reviewed the storage capacity after the reconstruction of gas reservoirs. Because the elastic expansion rate of rock and bound water was far lower than that of natural gas (generally $2 - 3$ orders of magnitude smaller than that of natural gas), the influence of the elastic expansion rate of rock and bound water was ignored. Yu et al. [35] investigated the pressure wave propagation velocity by gas reservoir engineering and numerical simulation, determined the buffer distance and accurately evaluated the UGS capacity. Tang et al. [36] simplified the original gas-bearing reservoir into water flooded zone, transition zone and pure gas zone, respectively, given the calculation formula of original gas-bearing pore space loss in each region, and introduced physical property zoning parameters to characterize reservoir heterogeneity, and established the material balance equation considering gas-bearing pore space loss and reservoir heterogeneity. Lai et al. [37] uses the material balance method to evaluate CO_2 storage capacity.in depleted wet/dry gas reservoirs. Wang et al.[38] established a dynamic unstable flow analysis method considering complex factors such as multi-period injection-production historical dynamics of gas reservoirs, and drew a relevant theoretical chart based on the characteristics of injection-production operation of strong heterogeneous gas reservoirs. The new method realizes the dynamic unsteady flow analysis of injection-production of UGS, and the storage capacity

fitting accuracy is high. At present, there is still a lack of calculation of gas storage capacity with cushion gas, so it is very meaningful to study the gas storage capacity under different cushion gas volume.

In this paper, we will use the material balance method to calculate the hydrogen storage capacity with CO_2 as cushion gas in depleted gas reservoirs, considering three gases in gas reservoirs: natural gas, CO_2 and H_2. The general sketch diagram of the method used in this study is shown in Fig. 2.

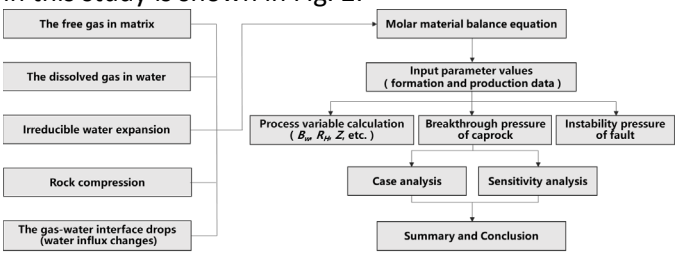

Fig. 2 General sketch diagram of the study problem

2. UHS POTENTIAL EVALUATION MODEL CONSIDERING CO_2 AS CUSHION GAS

2.1 Subdivision - numbered sections

In this paper, the basic assumptions for the derivation of the material balance equation are: (1) The reservoir physical properties and fluid physical properties of gas reservoirs are evenly distributed; the formation pressure at each point of the gas reservoir is in equilibrium at the same time, that is, the equivalent pressure at each point is equal; (2) When considering water-soluble gas, natural gas is dissolved in bound water and water body under the initial formation conditions, and its properties are the same as free gas. There are both free gas and water-soluble gas in the produced natural gas; (3) Gas mixing is small and not considered; (4) The change of stratum structure in the process of UHS operation is not considered.

Under these assumptions, the porous media system for the UHS can be simplified as an underground container for gas storage, as shown in Fig. 3. In this underground container, with the cyclic injection of gas reservoir, the volume change of gas and water obeys the principle of material conservation, which can establish the material balance equation of gas reservoir.

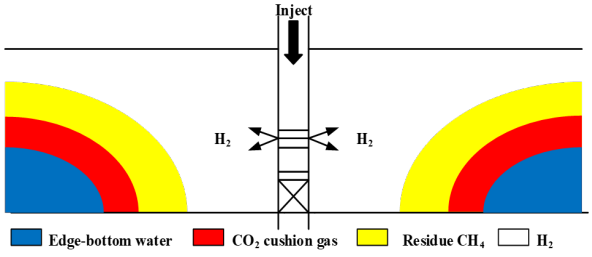

Fig. 3 Gas migration during UHS injection

As a result of gravity differentiation, the gas will be stratified (Fig. 4). We will treat the three gases in layers and the mixed part will not be considered.

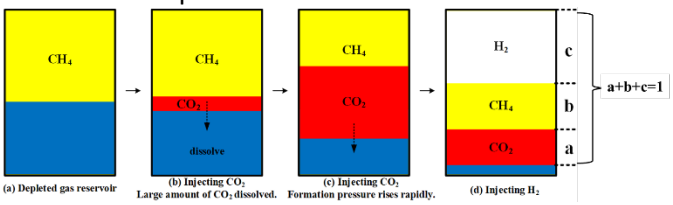

Fig. 4 The stage of injection about CO_2 as cushion gas and H_2 gas in the porous media of depleted gas reservoir

Considering the water-soluble gas, the molar conservation relationship of CO_2 and H_2 is: molar quantity under standard conditions= molar quantity under formation conditions; the residual gas in the depleted gas reservoir will be used as cushion gas: the molar quantity of natural gas in the depleted gas reservoir = the molar quantity of natural gas in the gas reservoir after injecting. Eq. (1) to (3) are the equilibrium equations of H_2-CO_2-CH_4 multicomponent substances.

$$\frac{p_{sc}V_{CO_2\_inj}}{Z_{sc}RT_{sc}}=\frac{pV_{CO_2}}{Z_{CO_2}RT}+\frac{p_{sc}V_{CO_2\_dis}}{Z_{sc}RT_{sc}} \tag{1}$$

$$\frac{p_{dep}V_{H\_dep}}{Z_{H\_dep}RT_{dep}}+\frac{p_{sc}V_{dep\_dis}}{Z_{sc}RT_{sc}}=\frac{pV_H}{Z_HRT}+\frac{p_{sc}V_{H\_dis}}{Z_{sc}RT_{sc}} \tag{2}$$

$$\frac{p_{sc}V_{H_2\_inj}}{Z_{sc}RT_{sc}}=\frac{pV_{H_2}}{Z_{H_2}RT}+\frac{p_{sc}V_{H_2\_dis}}{Z_{sc}RT_{sc}} \tag{3}$$

The real-time gas-bearing pore space in the formation is:

$$V=V_i\left[1-c_{eff}\left(p_i-p\right)\right]+V_{w\_p}B_w-W_e \tag{4}$$

The effective compression factor is expressed as:

$$c_{eff}=\frac{c_f+\left(s_w+M\right)c_w}{1-s_w} \tag{5}$$

The gas-bearing pore space in the original formation is:

$$V_i=G_iB_i=G_i\left(\frac{p_{sc}}{Z_{sc}T_{sc}}\right)/\left(\frac{p_i}{Z_iT_i}\right) \tag{6}$$

In order to obtain the H_2 injection volume, it is necessary to calculate the proportion of the other two gases in the pore space. As shown in Fig. 4, excluding the water invasion space in the formation, the proportion of pore space occupied by CO_2 is “a”, that is:

$$V_{CO_2}=aV \tag{7}$$

The volume of CO_2 dissolved in the formation is:

$$V_{CO_2\_dis}=\left[\frac{V_i\left(S_w+M\right)}{\left(1-S_w\right)B_{wi}}-V_{w\_p}-\frac{aVS_w}{\left(1-S_w\right)B_w}\right]R_{CO_2} \tag{8}$$

Substituting Eq. (4) -Eq. (8) into Eq. (1), the proportion of CO_2 in the pore space will be calculated.

Similar to the calculation of the proportion of CO_2, the proportion of pore space occupied by CH_4 is “b”:

$$V_H=bV \tag{9}$$

The pore space of the depleted gas reservoir is:

$$V_{dep} = V_i\left[1 - c_{eff}\left(p_i - p_{dep}\right)\right] + V_{w\_p}B_{w\_dep} - W_{e\_dep} \quad (10)$$

The volume of CH_4 dissolved in the formation is:

$$V_{H\_dis} = \left[\frac{bVS_w}{\left(1-S_w\right)B_w}\right]R_H \quad (11)$$

The volume of CH_4 dissolved in in depleted gas reservoirs:

$$V_{dep\_dis} = \left[\frac{V_i\left(S_w + M\right)}{\left(1-S_w\right)B_{wi}} - V_{w\_p}\right]R_{H\_dep} \quad (12)$$

Substituting Eq. (9)-Eq. (12) into Eq. (2), the proportion of CH_4 in the pore space will be calculated.

After calculating the proportion of pore space occupied by CO_2 and CH_4, the amount of storage space retained for H_2 can be determined:

$$V_{H_2} = \left(1-a-b\right)V \quad (13)$$

The volume of H_2 dissolved in the formation is:

$$V_{H_2\_dis} = \left[\frac{\left(1-a-b\right)VS_w}{\left(1-S_w\right)B_w}\right]R_{H_2} \quad (14)$$

The calculated V_{H2_inj} value is the UHS capacity of the target depleted gas reservoir.

3. DETERMINE THE MAXIMUM PRESSURE THRESHOLD

Calculating the cap-rock breakthrough pressure and fault-slip pressure of the UHS based on the cap and fault properties of the target depleted gas reservoir to further estimate the maximum pressure threshold of the UHS.

3.1 Mechanical integrity of caprock

The most classical risk assessment method for shear failure of caprock is based on Mohr-Coulomb criterion in rock mechanics. The cap-rock breakthrough pressure is calculated by the following equation:

$$\chi = 1 - \frac{\left(\sigma_1 - \sigma_3\right)/2}{c\cos\phi + \left(\sigma_1 + \sigma_3\right)\sin\phi/2} \quad (15)$$

where, χ is the cap safety factor; when χ = 0, the shear failure occurs; The maximum and minimum effective principal stresses are the main factors affecting the risk of shear failure of caprock, which are closely related to the change of formation pressure.

3.2 Fault mechanical stability

Based on the study of gas reservoir geology, the rock mechanics parameters of caprock were obtained by indoor rock mechanics experiment technology and in-situ stress parameters were obtained by small-scale hydraulic fracturing test, and the risk degree of caprock damage was quantitatively evaluated by safety index (SF) to evaluate the integrity of caprock. The fault-slip pressure is calculated by the following equation:

$$ST = \frac{\tau_s}{\sigma_n} \quad (16)$$

$$\sigma_n = \frac{\sigma_1 + \sigma_3}{2} + \frac{\sigma_1 - \sigma_3}{2}\cos 2\alpha \quad (17)$$

$$\tau_s = \frac{\sigma_1 - \sigma_3}{2}\sin 2\alpha \quad (18)$$

where, ST is the fault slip trend index; when ST < 0.6, the fault is mechanically stable; when ST⩾0.6, the fault is at risk of slip; the larger the ST, the higher the risk of slip.

The cap-rock breakthrough pressure and the fault-slip pressure are compared, and the smaller one is the maximum pressure threshold of the UHS.

4. CASE STUDY

Well PL4 is in the southeast of Penglai area and it is suitable for gas storage: the surface environment is favorable and the distance from the production area is moderate; there is no large-scale fault in the area, which is far away from the outcrop of the sealing layer; the depth of gas storage target layer is more than 800m; the water body is small, and it will be conducive for production. Table 1 shows the geological parameters and production parameters of the gas reservoir controlled by this well.

Table 1 Gas reservoir formation and production parameters

Parameter	Value	Parameter	Value
G_i	8000×10^4 [m^3]	p_{dep}	15 [MPa]
p_i	37 [MPa]	V_{w_p}	84300 [m^3]
M	0.18	T_i	79[℃]
c_f	5.7583 [MPa^{-1}]	T_{dep}	79[℃]
c_w	4.21×10^{-4} [MPa^{-1}]	p_{sc}	0.101325 [MPa]
S_w	0.46	T_{sc}	20[℃]
m	10 [g/L]	W_{e_dep}	146166[m^3]
σz	70[MPa]	σ_H	55 [MPa]
c	10 [MPa]	σ_h	45 [MPa]
α	43 [°]	ϕ	11 [°]

For the utilization of the material balance equation, we need to calculate the solubility, gas deviation factor and formation water volume coefficient that change during injection, as shown in Fig. 5.

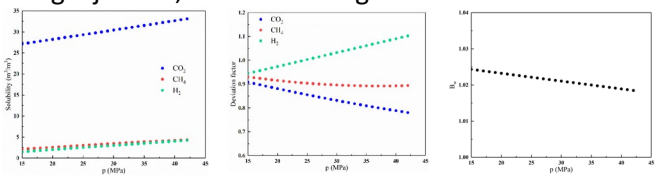

(a) (b) (c)

Fig.5 The variables that need to be calculated. (a) Solubility of CO_2, CH_4 and H_2; (b) Deviation factors of CO_2, CH_4 and H_2; (c) Formation water volume coefficient

As can be seen from Fig. 5, compared with the residual CH_4 and injected H_2, CO_2 has greater solubility in

formation water and better compressibility, which will have a positive impact on the construction of UHS. The designed formation pressure is 42MPa, calculated χ>0, and ST is less than 0.6. The safety risk is low, and it is within the scope of safety.

The model can obtain the values of CO_2 cushion gas volume and working gas volume. When V_{CO2_inj} is 3000×10^4 m^3, the final hydrogen storage capacity is 6792×10^4 m^3; When V_{CO2_inj} is 4000×10^4 m^3, the final hydrogen storage capacity is 6076×10^4 m^3; The more CO_2 cushion gas, the smaller the UHS capacity will be. With the injection of H_2, the ratio of natural gas and CO_2 in the formation is decreasing. Because of its stronger compressibility, the proportion of CO_2 decreases faster, and for cushion gas, it will provide more space for working gas.

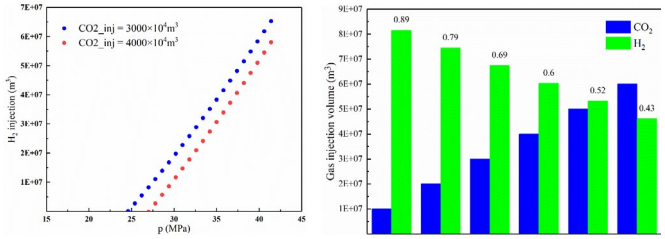

Fig.6 H_2 storage capacity when $V_{CO2\_inj} = 3000\times10^4$ m^3 and $V_{CO2\_inj} = 4000\times10^4$ m^3 (left); the injected volume of H_2 and the ratio of H_2 to the total injected gas volume under different CO_2 cushion gas volume.

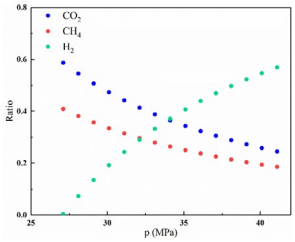

Fig. 7 Ratio of CO_2, CH_4 and H_2 to pore space in formation ($V_{CO2\_inj} = 4000\times10^4$ m^3)

5. MODEL COMPARISON

For water-bearing gas reservoirs, especially existing CO_2 injection, it is inevitable to consider solubility. In this model, the water multiple of gas reservoir is 0.18, and the dissolved gas in water will have a great influence on the hydrogen storage capacity of UHS. Ignoring the dissolution term in our material equation is the material balance equation without considering dissolution. The equation is calculated in the same way, and the results are compared as shown in Fig. 8.

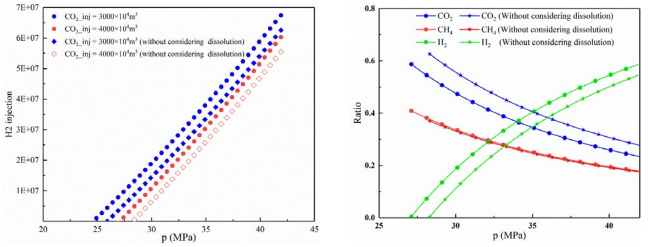

Fig.8 Comparison of hydrogen storage capacity considering dissolution and not considering dissolution (left) and Ratio of CO_2, CH_4 and H_2 to pore space in formation when $V_{CO2\_inj} = 4000\times10^4$ m^3 (right)

The UHS capacity will decrease without considering dissolution. When V_{CO2_inj} is $4000\times10^4 m^3$, the UHS capacity decrease by about 7.9% without considering dissolution. The proportion of CO_2 will become larger and the proportion of hydrogen will become lessened. It shows a situation similar to "hysteresis effect", in which the pore space occupied by hydrogen decreases.

6. SENSITIVITY ANALYSIS

Temperature and pressure are the main factors affecting the capacity of gas storage. In the process of UHS operation, the temperature of injected natural gas and the potential energy will change the temperature of the formation. The change of temperature for the parameters such as solubility, formation volume coefficient, gas deviation factor and so on. Of course, the change of the maximum pressure will also have a great impact on the gas storage capacity. We calculate the real-time hydrogen storage volume by changing the formation temperature and pressure respectively, and the result is shown in Fig. 9.

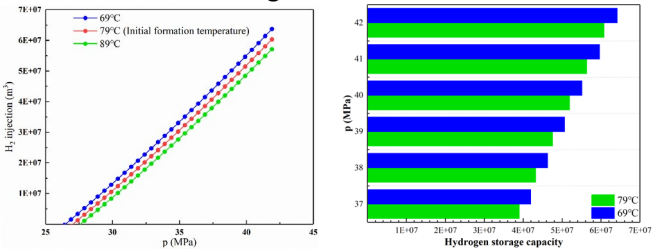

Fig.10 Comparison of hydrogen storage capacity at different temperatures when $V_{CO2\_inj}=4000\times10^4 m^3$ (left); H_2 storage capacity at different pressures of 69℃ and 79℃ (right)

As shown in Fig. 9, the decrease of formation temperature will increase the amount of the UHS capacity. $V_{CO2\_inj}=4000\times10^4 m^3$, compared with the initial formation temperature, the temperature drops by 10℃, and the hydrogen storage capacity increases by about 5.6%. The increase of the maximum pressure threshold will evidently expand the UHS capacity. The UHS capacity is less affected by temperature and more affected by formation pressure. However, it should be noted that

both temperature and pressure changes will have a great impact on reservoir safety under geological conditions.

7. CONCLUSIONS

Based on the law of conservation of molar matter, the material balance equation in the injection process of UHS considering CO_2 as cushion gas was established. We determine maximum pressure threshold by calculating the breakthrough pressure of caprock and the instability pressure of fault. The controlled UHS capacity of well PL4 is obtained. The change of gas volume ratio shows the superiority of CO_2 as cushion gas.

When CO_2 as cushion gas, especially in the presence of water, solubility is a factor that must be considered. Compared with the method without considering dissolution, the UHS capacity of the method will increase under the same cushion gas volume.

The decrease of formation temperature will increase the UHS capacity. Increasing the maximum pressure threshold will also increase the UHS capacity. Compared with change of temperature, the change of pressure has a greater influence on the expansion of UHS capacity.

ACKNOWLEDGEMENT

The authors gratefully acknowledge the Central Sichuan Division, Petro China Southwest Oil & Gas field Company for providing their data.

DECLARATION OF INTEREST STATEMENT

The authors declare that they have no known competing financial interests or personal relationships that could have appeared to influence the work reported in this paper. All authors read and approved the final manuscript.

REFERENCES

[1] Jin Zhao, A K Patwary, A Qayyum, et al. The determinants of renewable energy sources for the fueling of green and sustainable economy. Energy 2022;238 (C):122029.

[2] S F Ahmed, M Mofijur, S Nuzhat, et al. Sustainable hydrogen production: Technological advancements and economic analysis. Int. J. Hydrog. Energy 2022;47(88):37227-37255.

[3] Ibrahim Dincer, Canan Acar. Review and evaluation of hydrogen production methods for better sustainability. Int. J. Hydrog. Energy 2015; 40(34): 11094- 11111.

[4] Patrick Preuster, Alexander Alekseev and Peter Wasserscheid. Hydrogen Storage Technologies for Future Energy Systems. Annu Rev Chem Biomol Eng 2017;8:445-471.

[5] Sufang Zhang, Xingmei Li. Large scale wind power integration in China:Analysis from a policy perspective. Renew. Sust. Energ. Rev. 2012;16(2):1110-1115.

[6] Wang Y, Chao Q, Zhao L, et al. Assessment of wind and photovoltaic power potential in China. Carb Neutrality 2022;1:15.

[7] Junxia Liu. China's renewable energy law and policy:A critical review. Renew. Sust. Energ. Rev. 2019;99:212-219.

[8] National Energy Administration. Medium-and Long-term Planning for the Development of Hydrogen Energy Industry (2021-2035). 2022.

[9] Yuekuan Zhou. Transition towards carbon-neutral districts based on storage techniques and spatiotemporal energy sharing with electrification and hydrogenation. Renew. Sust. Energ. Rev 2022;162:112444.

[10] Jiang L, Fu X. An Ammonia-Hydrogen Energy Roadmap for Carbon Neutrality:Opportunity and Challenges in China. Engineering 2021;7(12):4.

[11] Joakim Andersson, Stefan Grönkvist. Large-scale storage of hydrogen. Int. J. Hydrog. Energy 2019;44(23):11901-11919.

[12] Davood Zivar, Sunil Kumar, Jalal Foroozesh. Underground hydrogen storage:A comprehensive review. Int. J. Hydrog. Energy 2021;46(45):23436-23462

[13] Wei Liu, Zhixin Zhang, Jie Chen, et al. Feasibility evaluation of large-scale underground hydrogen storage in bedded salt rocks of China: A case study in Jiangsu province. Energy 2020;198:117348.

[14] K Luboń & Tarkowski R. Influence of capillary threshold pressure and injection well location on the dynamic CO_2 and H2 storage capacity for the deep geological structure. Int. J. Hydrog. Energy 2021;46(58):30048-30060.

[15] Bahar M & Rezaee R. Impact of hydrogen solubility on depleted gas field's caprock for underground hydrogen storage purpose. APPEA 2021.

[16] L Lankof, K Urbańczyk, R Tarkowski. Assessment of the potential for underground hydrogen storage in salt domes, Renew. Sust. Energ. Rev. 2022;160:112309.

[17] Hemme C & Berk W. Hydrogeochemical modeling to identify potential risks of underground hydrogen storage in depleted gas fields. Appl. Sci. 2018;8(11), 2282.

[18] Bo Z, Zeng L, Chen Y, et al. Geochemical Reactions-Induced Hydrogen Loss During Underground Hydrogen Storage in Sandstone Reservoirs. Int. J. Hydrog. Energy 2021;46(38):19998-20009.

[19] Lysyy M, Fern A, & Ersland G. Seasonal hydrogen storage in a depleted oil and gas field. Int. J. Hydrog. Energy 2021;46(49):25160-25174.
[20] Feldmann, F., Hagemann, B., Ganzer, L. et al. Numerical simulation of hydrodynamic and gas mixing processes in underground hydrogen storages. Environ Earth Sci 2016;75:1165.
[21] Enigbokan T, Heinemann N & Li J. Application of CO_2 geologic storage experience to underground hydrogen storage reservoirs. Social Science Research Network. 2021.
[22] Anna S Lord, Peter H Kobos, David J Borns. Geologic storage of hydrogen: Scaling up to meet city transportation demands. Int. J. Hydrog. Energy 2014;39(28):15570-15582.
[23] T Bai, P Tahmasebi. Coupled hydro-mechanical analysis of seasonal underground hydrogen storage in a saline aquifer. J Energy Storage 2022;50:104308.
[24] Oldenburg C M. Carbon Dioxide as Cushion Gas for Natural Gas Storage. Energy & Fuels 2002;17(1):240-246.
[25] Cao C, Liao J, Hou Z, et al. Utilization of CO_2 as Cushion Gas for Depleted Gas Reservoir Transformed Gas Storage Reservoir. Energies 2020;13:576.
[26] Rui-han Zhang, Sheng-nan Chen, Shu-yong Hu, et al. Numerical simulation and laboratory experiments of CO_2 sequestration and being as cushion gas in underground natural gas storage reservoirs.J Nat Gas Sci Eng 2021;85:103714.
[27] G. Wang, G. Pickup, K. Sorbie, E. Mackay. Numerical modelling of H2 storage with cushion gas of CO_2 in subsurface porous media: Filter effects of CO_2 solubility. Int. J. Hydrog. Energy 2022;47(67):28956-28968.
[28] M Kanaani, B Sedaee, M Asadian-Pakfar. Role of Cushion Gas on Underground Hydrogen Storage in Depleted Oil Reservoirs. J Energy Storage 2022;45:103783.
[29] Kim J, Choi J, Park K. Comparison of nitrogen and carbon dioxide as cushion gas for underground gas storage reservoir. Geosystem Engineering 2015;18(3): 163-167.
[30] Hagemann B, Rasoulzadeh M, Panfilov M, et al. Hydrogenization of underground storage of natural gas. Comput Geosci 2016;20:595–606.
[31] Pfeiffer W, Beyer C & Bauer S. Hydrogen storage in a heterogeneous sandstone formation:dimensioning and induced hydraulic effects. Petrol Geosci 2017;23(3): 315-326.
[32] Eddaoui N, Panfilov M, Ganzer L, et al. Impact of Pore Clogging by Bacteria on Underground Hydrogen Storage. Transp Porous Med 2021;139: 89-108.
[33] Zhenkai Bo, Maartje Boon, Hadi Hajibeygi, et al. Impact of experimentally measured relative permeability hysteresis on reservoir-scale performance of underground hydrogen storage (UHS). Int. J. Hydrog. Energy 2023;48: 13527-13542.
[34] Guangrong Yang, Yuanzhou Yu, Guangxiong Jia, et al. Calculating the Capacity of Underground Natural Gas Storage by Material Balance Method. Nat Gas Ind 2003;23(2):96-99.
[35] Shuming Yu, Tao Lu, Zhijun Liu, et al. Determination of underground gas storage capacity for local low permeability lithological gas reservoirs. Nat Gas Ind 2012;32(6):36-38.
[36] Ligen Tang, Jieming Wang, Fengjua Bai, et al. Inventory forecast in underground gas storage based on modified material balance equation. Pet Explor Dev 2014;41(4):480-484.
[37] Lai Y T, Shen C H, Tseng C C, et al. Estimation of Carbon Dioxide Storage Capacity for Depleted Gas Reservoirs. Energy Procedia 2015;76:470-476.
[38] Jieming Wang, Chun Li, Junchang Sun, et al. An analysis method of injection and production dynamic transient flow in a gas field storage facility. Pet Explor Dev 2022;49(1):156-165.